

The Penalty Immersed Boundary Method
and its Application to Aerodynamics

Yongsam Kim

A dissertation submitted in partial fulfillment

of the requirements for the degree of

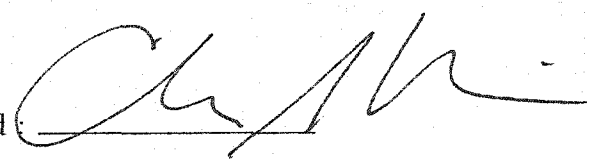
Doctor of Philosophy

Department of Mathematics

New York University

September 2003

Approved



Charles S. Peskin

UMI Number: 3105887

Copyright 2003 by
Kim, Yongsam

All rights reserved.

UMI[®]

UMI Microform 3105887
Copyright 2003 by ProQuest Information and Learning Company.
All rights reserved. This microform edition is protected against
unauthorized copying under Title 17, United States Code.

ProQuest Information and Learning Company
300 North Zeeb Road
P.O. Box 1346
Ann Arbor, MI 48106-1346

© Yongsam Kim

All Rights Reserved, 2003

PREVIEW

To my mother Kum-ja and my wife Juyoung

PREVIEW

Acknowledgements

I am happy to have this opportunity to express my gratitude to people without whom this work would not have been possible. First of all, I would like to thank my advisor, Charlie, not only for his invaluable advice on my research and work, but also for a great guidance in my life. It was the first time when I met him that I began learning and thinking about Applied Mathematics. With a great patience and support, he has been since then teaching and advising me. His tireless interest and ceaseless encouragement for my work will no question be a cornerstrone in both research and life of my future.

D.M.McQueen to whom I owe a great debt kindly shared his experience and knowledge of various aspects of the IB method. I have made extensive use of his 3-D visualization software in carrying out this work. I also thank E.Wolfszon for her effort to improve this software and to teach me to use it.

I am truely grateful to my mother Kum-ja who, in no exception, has been supportring me heartily and financially. My wife Juyoung, who is getting her Ph.D alongside me, has been always standing by me with her heart and mind. I am pretty sure she will be something in her area. I am also grateful to Juyoung's parents for their support and giving me great comfort.

I am grateful for support from the National Science Foundation under KDI research grant DMS-9980069.

Abstract

The Immersed Boundary (IB) method has been widely applied to problems involving a moving elastic boundary that is immersed in fluid and interacting with it. But most applications of the IB method have involved a massless elastic boundary. Extending the method to cover the case of a massive boundary has required spreading the boundary mass out onto the fluid grid and then solving the Navier-Stokes equations with a variable mass density. The variable mass density makes Fourier transform methods inapplicable, and requires a multigrid solver.

Here we propose a new and simple way to give mass to the elastic boundary. The key idea of the method is to introduce two representations of each boundary: one is a massive boundary which does not interact with the fluid, and the other is massless and plays the same role as the boundary of the IB method with the massless assumption. Although they are almost the same, we allow these two representations of the boundary to be different as long as the gap between them is small. This can be ensured by connecting them with a stiff spring with a zero rest length which generates force acting on both boundaries and pulling them together.

We call this the ‘Penalty IB method’. It does not spread mass to the fluid grid, retains the use of Fourier transform methodology, and is easy to

implement in the context of an existing IB method code for the massless case. This thesis introduces the Penalty IB method and applies it to several problems in which the mass of the boundary is important. These problems are filaments in a flowing soap film, flows past a cylinder, windsocks, flags, and parachutes.

PREVIEW

Contents

Dedication	iii
Acknowledgments	iv
Abstract	v
List of Figures	ix
List of Tables	xiv
1 Introduction	1
2 Equations of Motion	7
2.1 Outline of a Mathematical Derivation of the IB Method	8
2.2 Fluid-structure interaction	13
2.3 Equations of the Penalty IB Method	17
3 Numerical Implementation of the Penalty IB Method	27
3.1 Temporal discretization: 2nd order Runge-Kutta Method	28
3.2 Elastic force and spatial discretization	34

3.3	Numerical Penalty IB method	38
3.4	External Boundary Conditions	42
4	Applications of the Penalty IB Method to Aerodynamics	45
4.1	Flapping filament in a flowing soap film	46
4.2	Flow past a cylinder in 2-D	60
4.3	Windsock	73
4.4	Flag in wind and gravity	82
4.5	3-D Parachute	95
4.5.1	Construction of a model	95
4.5.2	Results: several kinds of parachute	102
5	Conclusions and Future Work	122
	Bibliography	125

List of Figures

2.1	Massive and massless boundaries are linked together with a very stiff spring of which the rest length is zero.	24
4.1	Initial setting of the filament simulation.	47
4.2	Maximum distance between massless and massive boundaries as a function of time.	51
4.3	y-component $V_0(t)$ of the desired inflow and the absolute error of the y-component of the calculated velocity $v(\mathbf{x}, t)$ from the desired velocity $V_0(t)$ at one specified point \mathbf{x}	52
4.4	x -coordinate of the free ends of two filaments in time.	55
4.5	Motion of two filaments with different mass densities: $10^{-5}\text{g}/\text{cm}^3$ and $4 \times 10^{-5}\text{g}/\text{cm}^3$	57
4.6	Motion of a filament with two different initial perturbations.	58
4.7	Vorticity contours for a filament with different initial perturbations	59

4.8 The disc in 2-D means an infinite cylinder in 3-D seen in one perpendicular plane. The circle (boundary) represents the massless boundary and the center is the massive boundary (point mass). They are connected by springs with their radius as a rest length.	63
4.9 Comparison of two methods for specifying the inflow velocity in the case of a dropped cylinder	66
4.10 The height of the disc $Y_p(t)$, the desired inflow velocity $V_0(t)$, and the force acting on the center $-\int \mathbf{F}_K(s, t)ds - Mge_2$	68
4.11 The Reynold number and the drag coefficient as functions of time.	71
4.12 Vorticity contours of flow past a freely falling cylinder are plotted at four different times.	72
4.13 Initial configuration of windsock and computational domain	74
4.14 The x-component $U_0(t)$ of the desired inflow, the absolute error of x-component of the induced velocity $u(\mathbf{x}, t)$ from the desired one $U_0(t)$ at one specified point \mathbf{x} , and the maximum distance (unit of meshwidth) between two boundaries.	78
4.15 Three different cases of a windsock are compared. Vorticity contours in a vertical plane that bisects the windsock are plotted.	79
4.16 Sideview of windsocks with different wind speeds: 5.0m/s and 2.5m/s.	80

4.17 The same situation as in Figure 4.16 with the view looking into the wind.	81
4.18 Initial configuration of a flag and the computational domain which is a box $1.28 \times 0.64 \times 0.64\text{m}^3$	83
4.19 Motions of a flag with and without wind.	85
4.20 Cartesian coordinates of the positions of three different material points on the downstream edge of the flag in time.	86
4.21 Motion of the massless flag. Even though all other conditions are same as in Figure 4.19 top, the massless flag neither flaps nor sags. See also Figure 4.22.	88
4.22 Comparison of the motions of two flags with and without mass .	90
4.23 Motion of a flag with a small wind speed. (time=2.4s)	91
4.24 Comparison of flag motions with low and high wind speed . .	92
4.25 Comparison of two flags with different initial perturbations .	94
4.26 Gore layout	96
4.27 Constructed profile of a parachute with canopy, payload (ball) and suspension lines	98
4.28 The inflation of a parachute	109
4.29 The inflation of a parachute from the top	110
4.30 The parachute and the trail of some fluid markers at a time=3.0s.	111

4.31 The same as Figure 4.30. Enlarged and seen from planes containing the middle of parachute.	112
4.32 Paracute falling with gravity to the ground which is a fixed no-slip boundary: time=0s (top) and 0.8s (bottom)	113
4.33 Continued from Figure 4.32: time=1.0s (top), 1.3s (top) and 1.6s (bottom).	114
4.34 Initial configuration of a three-canopy parachute	115
4.35 Comparison between one and three canopy parachutes with the force acting on the payload center (top), the height of the center (middle), and the inflow speed (bottom)	116
4.36 The three-canopy parachute and the trail of the surrounding fluid at a time=5.0s.	117
4.37 Continued. Enlarged and seen from a cross section inside the parachute.	118
4.38 Initial setting of 2 parachutes simulation	119
4.39 The motion of two parachutes and the trail of the surrounding fluid markers at fixed times: left-top=1.2s, right-top=2.4s, left-bottom=3.6s, and right-bottom=4.8s.	120

xiii

List of Tables

4.1	Parameters of flapping filament simulations	48
4.2	Parameters of the cylinder simulations	69
4.3	Parameters of the 3-D simulations	75
4.4	Construction parameters of a parachute	99
4.5	Parameters of parachute simulations.	102

Chapter 1

Introduction

We propose a simple way to extend the Immersed Boundary (IB) method to a situation in which an elastic moving boundary has mass that cannot be neglected and show several examples of the application of this new methodology. In the examples chosen, the boundary mass plays a crucial dynamical role.

The IB method was developed to study flow patterns around heart valves, and is a generally useful method for problems in which elastic materials interact with a viscous incompressible fluid. In the IB formulation, the influence of the elastic material immersed in the fluid appears as a localized body force acting on the fluid. This body force arises from the elastic stresses of the material. Moreover, the immersed material is required to move at the local fluid velocity as a consequence of the no-slip condition. The central idea of the

IB method is that the Navier-Stokes solver does not need to know anything about the complicated time-dependent geometry of the elastic boundary, and that therefore we can escape from the difficulties caused by the interaction between the elastic boundary and the fluid flow. This whole approach has been applied successfully to problems of blood flow in the heart and heart valves [19, 20, 21, 5, 6, 24, 26], wave propagation in the cochlea [10, 30], platelet aggregation during blood clotting [2], and several other problems [4, 9, 14, 15, 16, 17, 29, 32, 33, 35, 37, 38].

These applications, however, assume that elastic boundaries have no mass. The massless assumption appears in one version of the mathematical derivation of the IB method [23, 24, 26], see however [3, 37, 38], and can be applied when the mass of the moving boundary is too small to have a significant effect on the overall motions of the fluid and the elastic material. But with the massless assumption, we cannot approach many other problems that apparently need mass on the boundary.

For example, consider the simulation of a flapping filament in a flowing soap film as done by Zhu and Peskin [37]. This paper has shown that a massless filament does not flap at all, and that filament mass is essential for the sustained flapping that is seen not only in simulations with mass but also in laboratory experiments [36]. Subsequent experiments (J.Zhang, personal

communication) have shown as predicted that an extremely fine filament fails to flap under the same conditions in which flapping of a more massive filament had been seen. Many other examples, in which the massless assumption is not reasonable arise in aerodynamics. Since air is such a light fluid, it is usually the case that elastic boundaries immersed in air have mass that cannot be neglected. Not only the inertial effect of the boundary mass but also the effect of gravity on the boundary mass are important. We study several such examples in Chapter 4 of this thesis.

In [3, 37, 38], the method used to handle boundary mass was to spread that mass out onto the fluid grid, in much the same manner as boundary force is conventionally applied to the fluid grid in the IB computations. When this is done, a variable mass density $\rho(\mathbf{x}, t)$ appears in the Navier-Stokes equations, and this complicates the numerical solution of those equations. Specifically, it makes Fourier methods inapplicable and requires that an iterative method like Multigrid be used instead.

Our current approach stays much closer to the IB method for the massless case. In particular, it does not spread mass to the fluid and so it requires the same constant-density Navier-Stokes solver as is used in the massless case. The key idea is to introduce a massive boundary point as a twin of each immersed boundary marker where mass is needed. We assume that the massive boundary

thus introduced does not interact directly with the fluid and that the original immersed boundary, which will play the same role as in the original IB method, has no mass. The two boundaries are supposed to be the same, and when they move apart, a strong restoring force arises to pull them back together. This is done with a collection of stiff springs connecting the two boundaries. The massive boundary moves according to Newton's law ($F = ma$) in which the only forces acting are the forces of the stiff springs and the gravitational force. Meanwhile, at the other end of each spring, the massless boundary marker is moving at the local fluid velocity and spreading force locally to the fluid grid. Among the forces that it spreads is the force on the boundary marker due to the stiff spring (equal and opposite to the force acting on the massive boundary). Because the spring is stiff, the massive boundary point stays close to its twin immersed boundary marker, and the overall effect is that the boundary has mass.

Even though the two boundaries (which we call massive and massless boundaries) are supposed to coincide, we allow them to separate by an amount that depends inversely on the stiffness of the spring connecting them. The stiffness parameter of this spring is analogous to a penalty parameter in an optimization problem, which is why we call this new mass-handling idea the Penalty IB (pIB) method. We shall see later that, in the limit of infinite

spring stiffness, the two boundaries coincide, and the pIB method approaches the version of the IB method used by Zhu and Peskin [37, 38] for the massive case.

In order to validate the method, we first compare the filament simulation in a flowing soap film done by our method with Zhu's [37, 38]. From this comparison, we can see that the two ways of handling mass of the immersed boundary give similar results. Generalizing the 2-D filament to a 3-D problem, we do simulations of a flag with wind. One thing that makes the 3-D flag differ from the 2-D filament is the directions of the gravitational force and the wind. While both in the 2-D filament case have a same direction, the wind direction is perpendicular to the gravitational force on the 3-D flag. This difference induces much more complicated dynamics including not only the flapping but also the sagging motion of the flag.

For the second verification of the method, we calculate the drag coefficient of a flowing fluid around a cylinder, and compare it with data obtained from real experiments and other numerical simulations. In order to introduce the effect of mass, we drop the cylinder freely in a fluid flowing upward that prevents the cylinder from falling out of our computational domain. The drag from our method is little bigger than other data (especially, the real data), and the reason for this difference will be discussed. Additional 3-D applications of

the pIB method considered in this thesis are windsocks and parachutes. The parachute simulations include interactions between two or more parachutes, sometimes falling separately and sometimes attached to the same payload.

The outline of this thesis is as follows: In Chapters 2 and 3, we introduce the mathematical derivation and numerical scheme of the pIB method. Chapter 4 shows the models of application examples and their simulation results obtained by the pIB method. Conclusions and future work are discussed in Chapter 5.

PREVIEW

Chapter 2

Equations of Motion

We now derive the mathematical formulation of the pIB method. Since the pIB method is a modified version of the original IB method, we first summarize the basic idea of the IB method and a procedure for deriving its mathematical formulation [23]. Though these equations of motion derived are true for viscoelastic incompressible materials filling all of space, we are generally interested in the situation in which only certain (2-D) surface is filled by the viscoelastic material and the rest by a viscous incompressible fluid. We discuss in Section 2.2 on the change of the general formula into the specific one which is used in most application problems. Finally, we modify the formula for the IB method to introduce the pIB method which can be applied to the cases in which the mass of the immersed elastic material cannot be neglected.

2.1 Outline of a Mathematical Derivation of the IB Method

The mathematical derivation of the IB method is well explained in a Peskin's paper [23] and can be summarized as follows: (1) Take a Lagrangian energy functional of the state of the elastic material in terms of Lagrangian variables, (2) Using the least action principle, derive the equation of motion, (3) In applying the principle, change Lagrangian variables into Eulerian variables by making convolutions with the Dirac delta function. The aim of this derivation is to make the equations for motion of an elastic material look as much as possible like the equations of fluid dynamics. Once we have done that, the fluid-elastic structure interaction will be easier to handle.

Consider an elastic incompressible material filling 3-D space. Let (q, r, s) be curvilinear coordinates attached to the material so that fixed values of (q, r, s) label a material point. Let $\mathbf{X}(q, r, s, t)$ be the position at time t in Cartesian coordinates of the material point whose label is (q, r, s) . Let $M(q, r, s)$ be the mass density of the material in the sense that $\int_{\Gamma} M(q, r, s) dq dr ds$ is the mass of the part of the material defined by $(q, r, s) \in \Gamma$. Note that M is independent of time, since mass is conserved.

Note that $\mathbf{X}(\cdot, \cdot, \cdot, t)$ describes the configuration in space of the whole ma-

terial at the particular time t . We assume that this determines the elastic potential (stored) energy of the material according to an energy functional $E[\mathbf{X}]$ such that $E[\mathbf{X}(\cdot, \cdot, \cdot, t)]$ is the elastic energy stored in the material at time t . And we assume that the functional E is Fréchet differentiable, i.e., that there exists a function $-\mathbf{F}(q, r, s, t)$ called the Fréchet derivative such that

$$\Delta E[\mathbf{X}(\cdot, \cdot, \cdot, t)] = \int -\mathbf{F}(q, r, s, t) \cdot \Delta \mathbf{X}(q, r, s, t) dq dr ds, \quad (2.1)$$

where $\Delta \mathbf{X}$ is the perturbation from the configuration $\mathbf{X}(\cdot, \cdot, \cdot, t)$ and $\Delta E[\mathbf{X}]$ is the resulting energy perturbation to first order. (Instead of Δ , mathematicians traditionally use δ , which we reserve to use for the Dirac delta function.) As shorthand for (2.1) we shall in the future write $\mathbf{F} = -\Delta E/\Delta \mathbf{X}$.

The principle of least action states that our system will evolve over the time interval $(0, T)$ in such a manner as to minimize the action S defined by

$$S = \int_0^T L(t) dt, \quad (2.2)$$

where L is the Lagrangian (defined below). The minimization is to be done subject to given initial and final conditions and also to the constraint of incompressibility:

$$\mathbf{X}(q, r, s, 0) = \mathbf{X}_0(q, r, s), \quad (2.3)$$

$$\mathbf{X}(q, r, s, T) = \mathbf{X}_T(q, r, s), \quad (2.4)$$